Integral equation studies of charged colloids: non-solution boundaries and bridge functions

2003 J. Phys.: Condens. Matter 15 S3491

(http://iopscience.iop.org/0953-8984/15/48/010)

INSTITUTE OF PHYSICS PUBLISHING JOURNAL OF PHYSICS: CONDENSED MATTER

J. Phys.: Condens. Matter **15** (2003) S3491–S3507 PII: S0953-8984(03)66487-8

Integral equation studies of charged colloids: non-solution boundaries and bridge functions

Juan A Anta[1], **F Bresme**[2] **and Santiago Lago**[1]

[1] Departamento de Ciencias Ambientales, Universidad Pablo de Olavide, Carretera de Utrera, Kilometro 1, 41013 Sevilla, Spain
[2] Department of Chemistry, Imperial College London, Exhibition Road, London SW7 2AZ, UK

Received 21 July 2003
Published 20 November 2003
Online at stacks.iop.org/JPhysCM/15/S3491

Abstract

We calculate colloid–colloid correlations using an integral equation theory recently introduced to study charged colloidal suspensions (Anta and Lago 2002 *J. Chem. Phys.* **116** 10514). Colloid–ion, colloid–colloid and ion–ion correlations are treated using different levels of approximation. The colloid–ion direct correlation function (DCF) is obtained initially from a given colloid–colloid pair structure by solving the corresponding hypernetted-chain (HNC) integral equation. It is then used to formulate an effective colloid–colloid pair potential for which the one-component reference hypernetted chain equation (RHNC) is solved. This strategy is used to compute self-consistent colloid–ion and colloid–colloid correlation functions. Ion–ion correlations are considered within the mean spherical approximation and are uncoupled from the others. The present method converges faster and is numerically more stable than traditional multi-component HNC/RHNC integral equation approaches, and provides accurate results for all correlation functions for a wide range of thermodynamic states. Moreover, it exhibits a larger solution region than the ordinary HNC equation for charged systems. Results in the proximity and within the 'HNC' non-solution boundary are discussed. We find that the onset of non-solution behaviour for the present theory appears when the surface charge density of the colloidal particle is very large. To understand the origin of the non-solution line and to address the effect of multi-body interactions in colloid–colloid interactions, we have extracted 'empirical' bridge functions from molecular dynamics simulations of charged colloidal suspensions with charge asymmetries 20:2 and 60:1 and states close to the non-solution region. The colloid–colloid bridge functions exhibit attractive features at intermediate colloid–colloid distances, whereas the colloid–ion bridge function is strongly attractive in the proximity of the non-solution boundary. These attractive components cannot be accounted for by either the hard-sphere bridge function or the first resummed (second order in density) bridge diagrams.

(Some figures in this article are in colour only in the electronic version)

0953-8984/03/483491+17$30.00

1. Introduction

In a recent paper [1], two of the present authors proposed an integral equation theory aiming to describe efficiently the colloid–colloid structure while taking into account the multi-component nature of the colloidal suspension. This approach is based on an iterative, self-consistent procedure, which permits us to obtain readily an effective pair potential between colloids. The evaluation of the effective potential between colloidal particles is a key ingredient to interpret the microscopic structure and the phase behaviour of colloidal suspensions [2]. Colloidal suspensions are multi-component systems characterized by a large asymmetry in size and charge. In this situation, the standard and most efficient way of dealing with the problem is by *coarse graining*, i.e., to eliminate the degrees of freedom of the smaller and less charged particles so that the mixture is treated as an effective one-component system (OCS) of large particles. The most prominent example of a coarse-graining procedure is the well known Derjaguin–Landau–Verwey–Overbeek (DLVO) theory and effective potential [3], widely used nowadays in colloidal science. The DLVO potential, obtained originally from Poisson–Boltzmann theory, can also be derived in the context of density functional theory (DFT) by integrating out the degrees of freedom of the small particles [4, 5]. Although this treatment leads to an effective potential which can be pairwise additive under certain approximations, integration of the degrees of freedom of the small particles in the total partition function does not produce an effective potential that is, *a priori*, pairwise additive. Moreover, as recently pointed out by Louis [6], an effective potential that leads to the right thermodynamics might not be adequate to describe the structure, and vice versa.

In the context of integral equation theories [7], a different route is normally followed to obtain the effective inter-colloidal potential [8]. In this case, the OCS is defined as a simple fluid which has the same colloid–colloid radial distribution function as the original mixture. The colloid–colloid structure determines a single interaction potential between colloids which is pairwise additive by definition. This is based on Henderson's theorem [9] which establishes that, in any many-body homogeneous system at a given global density, there is a one-to-one correspondence between $g(r)$ and a pair potential $u(r)$. The effective potential so obtained not only leads to the right colloid–colloid structure (by definition), but it can be used to evaluate the thermodynamic properties provided the other radial distribution functions, colloid–counterion and counterion–counterion, are also known. In this paper we will follow this alternative approach.

In our previous paper we have also shown that it is not necessary to use the same level of approximation for all the correlations in a colloidal mixture. Thanks to the large asymmetry in size and charge, colloid–ion and ion–ion correlations can be adequately treated in the hypernetted-chain approximation (HNC) and in the mean spherical approximation (MSA) respectively [7, 10]. The most sophisticated closure relation, i.e., the reference hypernetted-chain (RHNC) theory, is used to describe the OCS only. It is shown [1] that this simplification leads to accurate colloid–colloid radial distribution functions and effective potentials, while reducing the numerical complexity of the problem. This method is totally analogous to a strategy that has been put forward in liquid metals [11] in the context of the so-called *quantum-hypernetted-chain* (QHNC) theory [12]. Several works discussing the use of this procedure in colloidal suspensions can be found in the literature [13]. Furthermore, a similar procedure has been used to describe the electrical double layer in planar geometries [14]. In this work, the authors utilize the HNC closure to treat the wall–ion correlations whereas ion–ion correlations are considered within the MSA approximation. We call our approach [1] 'coarse-grained' hypernetted chain (CGHNC) since this integral equation method represents an efficient way of eliminating the degrees of freedom of the small particles and it focuses only on the effective one-component system only.

In this paper we study the non-solution boundary of the CGHNC integral equation. We will show that the CGHNC equation has a solution for thermodynamic states where the ordinary HNC equation does not. Despite this improvement, the CGHNC cannot be solved either when the colloidal bare charge is very large or when the packing fraction of colloids becomes very small. We showed in our previous work [1] that, at fixed colloidal packing fraction, the magnitude that really determines whether the integral equations can be solved or not is the surface charge density of the colloidal particle. We have already suggested this can be related to the phenomenon of 'ionic condensation' [15], as a large surface charge density favours a strong electrostatic coupling at the colloidal surface. Ionic association is by no means exclusive of charged colloidal suspensions. Indeed, it is a general fact in electrolyte systems [16], and results in ionic cluster formation in the low-density–high-ionic-strength limit [17]. In fact, a condensation model for colloidal suspensions in the spirit of the Bjerrum association extension of the Debye–Hückel theory of electrolytes has been successfully applied to these systems [18]. New integral equation approaches based on association concepts have also been recently used to study ion–ion correlation in colloidal suspensions [19].

In this work we explore the capability of the integral equation formalism to surmount the deficiencies observed in previous theoretical approaches, in particular the multicomponent HNC theory. At this point it must be noted that the Ornstein–Zernike theory along with its 'closure relations' constitutes an exact formalism if the so-called bridge functions are known. Therefore, we expect that the ionic condensation effects should be manifested in the shape of the exact bridge functions. With this aim, we have extracted 'empirical' bridge functions from molecular dynamics simulations for thermodynamic states in the vicinity of the CGHNC integral equation non-solution line. We have then compared the results for the colloid–colloid bridge function with the hard-sphere bridge function that minimizes the total free energy of the mixture (in the spirit of the RHNC theory). In addition, we have incorporated into the OCS part of the CGHNC formalism the computation of the first diagrams (second order in density) of the colloid–colloid bridge function [20]. We will show that neither the hard-sphere bridge function, which is repulsive by definition, nor the first 'resummed' (written in terms of h-bonds) bridge diagrams, are capable of catching the attractive features observed in the 'empirical' bridge function.

The outline of the paper is as follows: in section 2 we briefly rewrite the derivation of the CGHNC theory and the numerical strategy used to implement it. In section 3 we analyse the performance of the CGHNC with respect to the ordinary multi-component HNC integral equation and we present results for the correlation functions, effective potentials and thermodynamic properties of colloid–counterion mixtures at thermodynamic states for which the ordinary multicomponent HNC theory does not have a solution. Comparison with molecular dynamics data is also included in this section. Section 4 reports 'empirical' bridge functions extracted from molecular dynamics simulations along with hard-sphere bridge functions and the first resummed bridge diagrams. Finally, in section 5 the main conclusions of this work are summarized.

2. The CGHNC theory

In the present work we consider a system of colloidal particles with positive charge z_c in the presence of negatively charged counterions of charge $-z_i$. The number density of the colloids is ρ_c whereas the density of the counterions is given by the charge electroneutrality condition, hence $\rho_i = -(z_c/z_i)\rho_c$. Colloids and counterions interact via pair potentials of the type

$$u_{mn}(r) = u_{mn}^{sr}(r) + \frac{z_m z_n e^2}{4\pi\varepsilon r}, \qquad (m, n = c, i) \tag{1}$$

where u^{sr} is a short-range interaction and ε is the permittivity of the solvent, which is taken as a continuum. In order to derive equations that conveniently describe our system we proceed as follows.

Step 1 (Many-body problem). In the integral equation formalism, many-body interactions are treated by means of the Ornstein–Zernike (OZ) equations [10]. For a binary mixture they can be written as [21]

$$\begin{aligned} S_{\mathrm{cc}}(k) &= [1 - \rho_{\mathrm{i}} C_{\mathrm{ii}}(k)]/D(k) \\ S_{\mathrm{ci}}(k) &= \sqrt{\rho_{\mathrm{c}}\rho_{\mathrm{i}}}\, C_{\mathrm{ci}}(k)/D(k) \\ S_{\mathrm{ii}}(k) &= [1 - \rho_{\mathrm{c}} C_{\mathrm{cc}}(k)]/D(k) \\ D(k) &= [1 - \rho_{\mathrm{i}} C_{\mathrm{ii}}(k)][1 - \rho_{\mathrm{c}} C_{\mathrm{cc}}(k)] - \rho_{\mathrm{c}}\rho_{\mathrm{i}}[C_{\mathrm{ci}}(k)]^2 \end{aligned} \tag{2}$$

where the $S_{mn}(k)$ (c = colloid, i = counterion) are the Ashcroft–Langreth partial structure factors [22]. These are related to the total correlation functions (TCFs) h_{mn} via

$$S_{mn}(k) = \delta_{mn} + (\rho_m \rho_n)^{1/2} \int_V \mathrm{d}\mathbf{r}\, \mathrm{e}^{\mathrm{i}\mathbf{k}\cdot\mathbf{r}} h_{mn}(r) = \delta_{mn} + (\rho_m \rho_n)^{1/2} h_{mn}(k), \tag{3}$$

with the $C_{mn}(k)$ being the direct correlation functions (DCFs). The OZ equations are exact relations between *all* TCFs, describing the pair structure of the system, and the second-order functional derivatives of the excess free energy represented by the DCFs [10, 11, 21]. In a one-component fluid, the OZ equations (2) reduce to the familiar form

$$S(k) = 1 - \rho h(k) = \frac{1}{1 - \rho C(k)}. \tag{4}$$

Step 2 (Coarse graining). As mentioned in the introduction, we reduce the problem to an effective one-component system (OCS) by taking [8, 11]

$$S(k) = S_{\mathrm{cc}}(k) \tag{5}$$

where $S(k)$ is the structure factor of the OCS. Thus, the OCS is defined as the fluid whose characteristic pair structure is identical to the colloid–colloid pair structure of the original two-component system. In this way, we make sure that the effective pair potential describing the OCS contains, by definition, all many-body contributions associated with the counter-ionic degrees of freedom via the OZ equations. The effective potential so constructed is then *state dependent* but pairwise additive by definition.

By combining equations (2), (4) and (5) we find the following relationship between the DCFs of the OCS and the mixture:

$$C(k) = C_{\mathrm{cc}}(k) + \frac{\rho_{\mathrm{i}}[C_{\mathrm{ci}}(k)]^2}{1 - \rho_{\mathrm{i}} C_{\mathrm{ii}}(k)}. \tag{6}$$

Step 3 (Effective potential). In order to find an expression for the interaction characteristic of the OCS, i.e. the effective potential, we utilize the same strategy as before but now applied to the pair distribution functions $g_{mn}(r) = h_{mn}(r) + 1$ and their corresponding potentials of mean force $w_{mn}(r)$ [10]

$$g(r) = \exp[-\beta w(r)] = g_{\mathrm{cc}}(r) = \exp[-\beta w_{\mathrm{cc}}(r)] \tag{7}$$

where $\beta = 1/k_{\mathrm{B}}T$. The potential of the mean force can be related in turn to the DCFs, hence

$$-\beta u^{\mathrm{eff}}(r) + h(r) - C(r) - B(r) = -\beta u_{\mathrm{cc}}(r) + h_{\mathrm{cc}}(r) - C_{\mathrm{cc}}(r) - B_{\mathrm{cc}}(r) \tag{8}$$

where $u^{\mathrm{eff}}(r)$ is the effective potential and the B_{mn} are the so-called *bridge functions*. The bridge functions are related to the 'higher-than-two' functional derivatives of the excess free energy functional with respect to the density profiles [21]. Neglecting their contribution leads

to the well known HNC approximation [21]. In contrast, by including them in equation (8), we start from an approach that is formally exact. We next make use of equation (6) to arrive at the following expression for the effective pair potential between colloids[3]

$$\beta u_{\rm eff}(r) = \beta u_{\rm cc}(r) - \int C_{\rm ci}(k)\chi_{\rm ii}(-k)C_{\rm ci}(-k)\,{\rm d}\mathbf{k} + [B_{\rm cc}(r) - B(r)]$$
$$= \beta u'_{\rm eff}(r) + [B_{\rm cc}(r) - B(r)] \tag{9}$$

with

$$\chi_{\rm ii}(k) = \frac{\rho_{\rm i}}{1 - \rho_{\rm i}C_{\rm ii}(k)}, \tag{10}$$

which is the *linear-response* function of the fluid of counterions. Equation (9) shows that the effective interaction $u'_{\rm eff}(r)$ between colloidal particles is made up of two contributions: (1) direct Coulombic repulsion and (2) counterion-mediated attraction between colloids and the ionic 'atmosphere' of neighbouring colloids, this 'atmosphere' being represented by the counterion density profile around a colloidal particle $n_{\rm ci}(k) = \chi_{\rm ii}(k)C_{\rm ci}(k)$. This is exactly analogous to the expression for the effective potential between positive metallic ions in liquid metals [10] if we regard the colloid–counterion DCF as an ion–electron *pseudopotential* [11, 12]. The only difference is that in the present case the *background* fluid (electrons in liquid metals, counterions in colloidal suspensions) is not of a quantum nature and therefore can be treated on the same grounds as the rest of the components of the fluid.

Step 4 (Counter-ionic background). The expression introduced above for the effective potential depends on the counterion–counterion correlations via the response function, which in turn depends on the DCF. In the present approach, we choose a simple expression for this DCF,

$$\text{Approximation 1: } C_{\rm ii}(r) = \begin{cases} -\beta u_{\rm ii}(\sigma_{\rm i})\gamma(\rho_{\rm i},\sigma_{\rm i}) & r < \sigma_{\rm i} \\ -\beta u_{\rm ii}(r) & r > \sigma_{\rm i}, \end{cases} \tag{11}$$

where $\sigma_{\rm i}$ is the diameter associated with the counterions and γ is a constant parameter that is chosen such that $C_{\rm ii}$ is continuous at $r = \sigma_{\rm i}$ and consistent with the condition of excluded volume for the colloidal cores. Following the DFT treatment of van Roij *et al* [4], we make the following choice for γ:

$$\gamma(\rho_{\rm i},\sigma_{\rm i}) = \left(\frac{\kappa_{\rm D}\sigma_{\rm i}}{1 + \kappa_{\rm D}\sigma_{\rm i}}\right) \tag{12}$$

with $\kappa_{\rm D}$ being the inverse Debye length, i.e.

$$\kappa_{\rm D}^2 = \frac{4\pi\rho_{\rm i}z_{\rm i}^2}{k_{\rm B}T\varepsilon}. \tag{13}$$

Note that, by using this approximation, we make the counterion–counterion direct correlation function *independent* or *uncoupled* from the rest of the correlations in the mixture. In other words, we assume that colloids move in a sea of counterions and interact with them with a response function that behaves as if the colloids were absent. Also, this procedure implies treating counterion–counterion interactions in the *mean spherical approximation* (MSA) [10], i.e., excluded volume condition at short distances plus equivalence between interaction

[3] It must be noted that in our previous paper [1], the effective potential did not contain any bridge-function contribution as it was assumed that the colloid–colloid bridge function and the one-component bridge function were essentially identical. We will show later that this approximation is not needed to formulate the CGHNC theory. The effective potential defined in our previous work corresponds to what we denote here by $u'_{\rm eff}(r)$.

potential and DCF at long distances. By using this simplification we reduce the numerical complexity of the integral equation without reducing its accuracy. Hence, we will show later that we get very precise results not only for the colloid–colloid and colloid–counterion radial distribution functions, but also for the counterion–counterion structure itself.

Step 5 (Colloid–counterion correlation). We treat this interaction in the HNC approximation, which means that the colloid–counterion mean-force potential is obtained through

$$\text{Approximation 2: } w_{\mathrm{ci}}(r) = \beta u_{\mathrm{ci}}(r) - h_{\mathrm{ci}}(r) + C_{\mathrm{ci}}(r). \tag{14}$$

This equation is solved in conjunction with the colloid–counterion part of the OZ equations (2)

$$h_{\mathrm{ci}}(k) = C_{\mathrm{ci}}(k) + \rho_{\mathrm{c}} C_{\mathrm{ci}}(k) h_{\mathrm{cc}}(k) + \rho_{\mathrm{i}} C_{\mathrm{ii}}(k) h_{\mathrm{ci}}(k), \tag{15}$$

where C_{ii} is given by equation (11) and h_{cc}, which describes the colloid–colloid pair structure, is an *input* to this part of the problem. In other words, the distribution of counterions around a colloidal particle is obtained by solving the multi-component HNC equation for a given, *fixed*, colloid–colloid pair distribution. As shown in [1], this choice proves to be more adequate than linearized Poisson–Boltzmann theory to describe the colloid–counterion structure a finite density of colloids.

Step 6 (Solution of the effective colloid–colloid problem). Once we have solved the colloid–counterion correlation, and obtained $C_{\mathrm{ci}}(r)$, the effective potential between colloids is completely determined via equations (10)–(12). In the OCS, this potential induces a colloid–colloid pair structure that is obtained using the RHNC approximation:

$$\text{Approximation 3: } w(r) = \beta u'_{\mathrm{eff}}(r) - h(r) + C(r) + B^0_{\mathrm{cc}}(r; D), \tag{16}$$

where $u'_{\mathrm{eff}}(r)$ is defined in equation (9) and B^0_{cc} is the bridge function of a *reference* hard-sphere system [23]. This depends parametrically on the hard-sphere diameter D. As the mean-force potential is directly related to the $h(r)$ via $h(r) = \exp[-w(r)] - 1$, the colloid–colloid pair structure is completely determined, for a given D and effective potential, by equation (16) coupled with the one-component OZ equation (4). Alternatively, the bridge function can be ignored in equation (16), such that the HNC approximation is also applied in the colloid–colloid problem. As we will see below, this provides a good first approximation of both the colloid–colloid and colloid–counterion correlations.

2.1. General strategy and numerical details

Both steps 5 and 6 consider the solution of an integral equation for only one correlation, keeping the rest fixed. In view of this, we iterate over steps 5 and 6 until self-consistency is achieved. The result should be equivalent to the solution of the full multi-component OZ equations with MSA, HNC and RHNC closures for the counterion–counterion, colloid–counterion and colloid–colloid correlations respectively.

The whole formalism still depends parametrically on a single parameter, the hard-sphere diameter D. In our previous work we optimized D by requiring thermodynamic consistency [24] between the *total* pressure obtained from the compressibility route and the virial route. Nonetheless, we have found that it is more robust to vary D until the total HNC free energy of the mixture [23, 24] reaches a minimum.

The HNC and RHNC integral equations are solved numerically on a grid of 4096–16 384 points with a grid size of 0.01–1 nm in real space. The method of Ng [25] combined with Broyles' strategy [26] to mix conveniently successive estimates of the correlation functions is employed to enhance the convergence in the numerical solution of each integral equation. As regards the full CGHNC self-consistent procedure, we start from the HNC solution of the

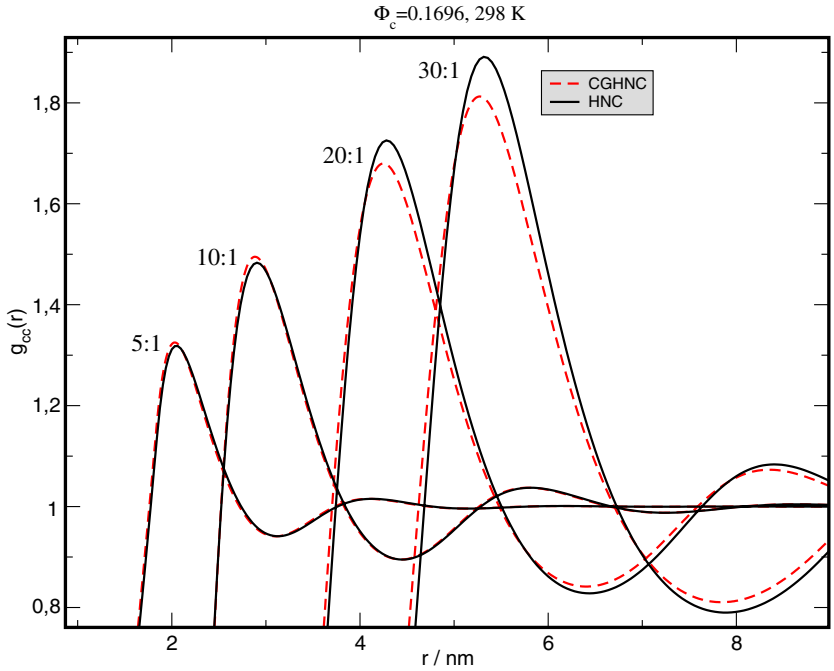

Figure 1. Colloid–colloid radial distribution functions for hard-core colloid–counterion mixtures as defined in table 1. Results predicted by the CGHNC and HNC theories are included in the graph as well as the charge asymmetries for which these results were obtained.

OCS described by the standard DLVO effective potential. Self-consistency is then obtained normally in a few successive iterations of steps 5 and 6. As mentioned above, when solving the OCS in the RHNC approximation, different values of D are tested until the total HNC free energy of the mixture is minimized.

3. Microscopic structure and effective potentials

3.1. CGHNC versus ordinary HNC

In order to check the performance of the CGHNC as compared with the standard HNC theory for mixtures, we have solved both theories for systems of increasing charge asymmetry. In order to make the comparison as significant as possible, we have kept the total packing fraction and the colloidal surface charge density equal in all cases. The parameters that define the system as well as the results obtained for the virial pressure and excess free energy can be found in table 1. Also, the colloid–colloid radial distribution functions are plotted in figure 1. It must be noted that in these calculations the OCS in the CGHNC equations (equation (17)) are treated in the HNC approximation, i.e., no colloid–colloid bridge functions were introduced. Otherwise, the comparison between the two theories would not be consistent.

The first conclusion to be extracted from this comparison is that, in spite of the approximations considered in the derivation of the CGHNC equations, the theory leads to very similar results to those obtained from the solution of the full HNC equations. The comparison is somewhat worse for the system with the largest charge asymmetry (30:1) because in this case the colloidal structure is much more pronounced and, therefore, the MSA approximation

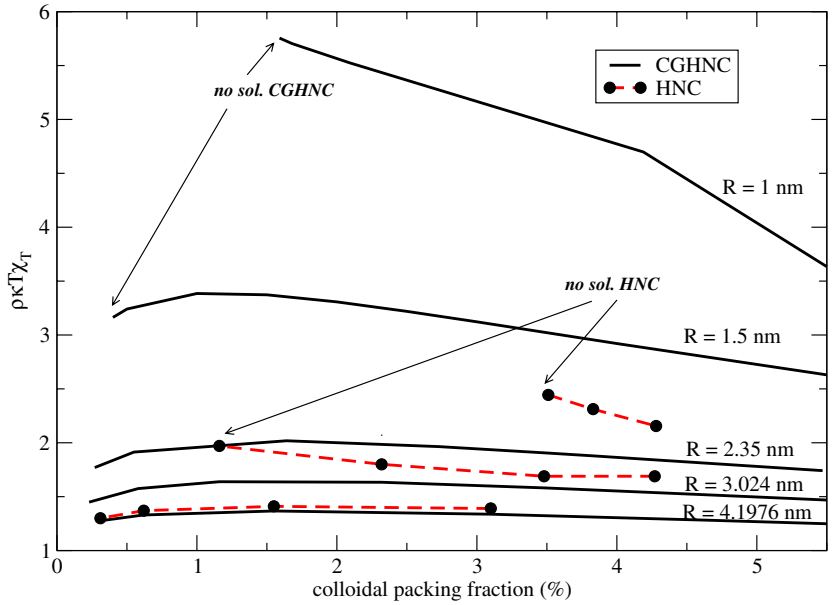

Figure 2. Total isothermal compressibility versus colloidal packing fraction for colloid + counterion mixtures with pointlike monovalent counterions at 298 K with colloidal charge $Z = 20$ and colloidal radii as shown. HNC results are from [16] and CGHNC results are obtained with the OCS treated in the HNC approximation (see the text for details).

Table 1. Parameters of hard-core colloid–counterion mixtures (with monovalent counterions) and thermodynamic results, pressure (P) and excess free energy (A), from CGHNC and standard HNC theories.

				CGHNC		HNC	
ρ_c (nm^{-3})	Z_C/electrons	σ_c (nm)	σ_i (nm)	$P/\rho kT$	A^{ex}/NkT	$P/\rho kT$	A^{ex}/NkT
0.096	5	1.5	0.32	1.22	−1.24	1.25	−1.12
0.035	10	2.1	0.35	1.01	−2.11	1.06	−2.02
0.012	20	3	0.4	0.83	−3.20	0.84	−3.25
0.006 53	30	3.67	0.4	0.74	−4.06	0.78	−4.09

becomes inaccurate treating counterion–counterion correlations. Nonetheless, the CGHNC converges much faster that the full HNC integral equation and it can provide accurate results for thermodynamic states for which the multicomponent HNC does not have a solution.

In order to show the numerical advantages of the present integral equation theory, we have solved the CGHNC equations for hard-core colloid–counterion mixtures with pointlike monovalent counterions (see figure 2). This case was already studied by Belloni with the standard multi-component HNC equations [16]. A most prominent feature of our calculations is that the CGHNC equations can be solved at much lower packing fractions and much larger surface charge densities than the ordinary HNC. As we showed in [1], the CGHNC integral equation becomes increasingly more unstable with increasing surface charge densities. This is also true for the ordinary HNC. What we can observe here is that the CGHNC improves in this respect upon the HNC approach. This improvement is by no means spurious or artificial. As we will show below by comparison against molecular dynamics simulations, the CGHNC theory

provides accurate results for thermodynamic states for which the ordinary HNC does not have a solution. Theories that introduce association ideas [19], i.e. the associated HCN (AHNC), also improve with respect to the traditional multicomponent HNC integral equation. Unfortunately there are not systematic studies on the non-solution region, and therefore it is not possible to establish a full comparison on whether our theory extends further the non-solution region. The AHNC gives solutions for colloidal suspensions down to 0.001 M and colloid radius 1.5 nm. This corresponds to ∼0.85% packing fraction. According to figure 2, the CGHNC theory can extend the solution range below 0.5%.

3.2. CGHNC versus molecular dynamics: colloid–counterion mixtures with charge asymmetry 60:1 and 60:2

In this section we present results for two systems for which the ordinary multi-component HNC equation does not have a solution. In these calculations the short-range potential in equation (1) is taken to be [27]

$$u_{mn}^{\mathrm{sr}}(r) = F_{mn}/r^9 \tag{17}$$

with F_{mn} chosen such that the minimum in the total soft-core potential coincides with that in the corresponding hard-core one, that is, $F_{mn} = -z_m z_n e^2 \sigma_{mn}^8/(9\varepsilon)$. We have chosen $\sigma_{\mathrm{cc}} = 4$ nm, $\sigma_{\mathrm{ci}} = 2.2$ nm and $\sigma_{\mathrm{ii}} = 0.4$ nm. The density of colloidal particles is taken as $\rho_{\mathrm{c}} = 0.002\,\mathrm{nm}^{-3}$. The simulations involved typically 3×10^5 time steps, with a time step of 0.01 ps and 5×10^4 steps of equilibration, and were performed in the Nosé–Hoover ensemble using the DL_POLY package [28]. The simulations were run in parallel in the HPCx supercomputer at the University of Edinburgh (UK) using 32 nodes. Results for the colloid–colloid, colloid–counterion and counterion–counterion radial distribution functions can be found in figures 3 and 4.

Comparison with simulation results shows that the CGHNC is very accurate in reproducing the colloid–counterion $g(r)$. As for the colloid–colloid structure this is only well described if a hard-sphere bridge function with optimized hard-sphere diameter is introduced in the solution of the OCS (see equation (16)). The counterion–counterion structure deserves a separate comment. As stated above, in the CGHNC procedure the counterion–counterion correlations are not solved self-consistently with the rest of the correlations. On the contrary, they are kept uncoupled and treated with the simplest approximation, i.e., the MSA. Therefore, it is not expected to achieve good agreement with exact simulation results for these correlations. Nevertheless, once a convergent CGHNC solution is obtained, it is possible to invert the OZ equations and extract the counterion–counterion correlations from the rest. We report the result obtained in this way in the lower part of figures 3 and 4. We can see that, despite the simplification intrinsic to the CGHNC procedure, the counterion–counterion radial distribution function accurately reproduces the molecular dynamics results. This fact proves that introducing approximation 1 in equation (12) firstly reduces the numerical complexity of the integral equation, and secondly leads to an accurate description of the mixture.

In table 2 we also report the thermodynamic properties for the suspensions discussed above. The agreement between CGHNC and molecular dynamics is very good, in particular for the 60:1 mixture. For the 60:2 case, we observe that the introduction of a hard-sphere bridge function with optimized diameter somewhat deteriorates the results. This could be a consequence of a larger relative contribution of the counterion–counterion correlations, which, as explained above, is not obtained self-consistently with the rest of the correlations.

It is also interesting to check the effective colloid–colloid pair potentials. These can be obtained self-consistently in the context of the CGHNC equations. The results for the 60:1 and 60:2 cases are presented in figure 5. We have also included in this graph the results for

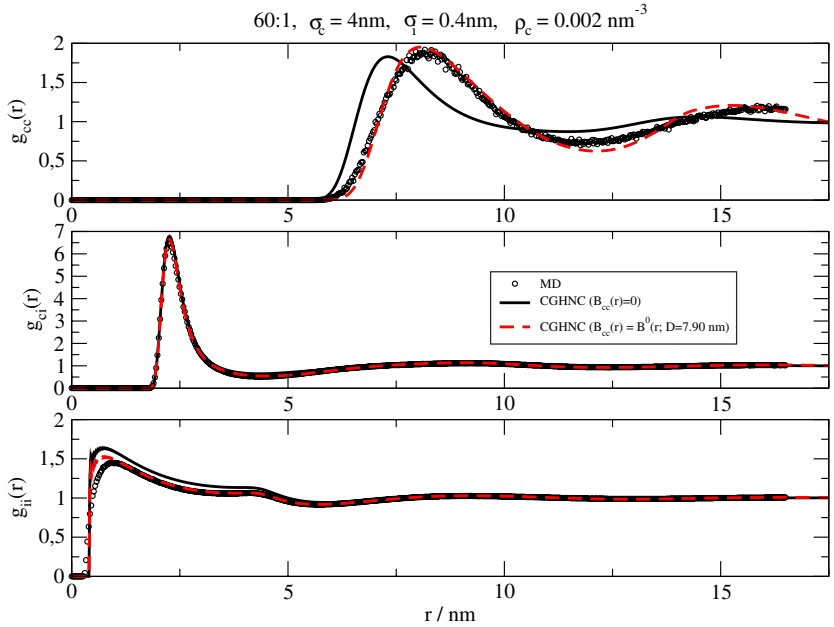

Figure 3. Radial distribution functions for soft-core mixtures of colloid and monovalent counterions with $\sigma_{cc} = 4$ nm, $\sigma_{ci} = 2.2$ nm and $\sigma_{ii} = 0.4$ nm and density of colloidal particles $\rho_c = 0.002\,\mathrm{nm}^{-3}$ (see the text for details). White circles correspond to molecular dynamics results, solid curves refer to CGHNC predictions with the OCS treated in the HNC approximation (that is, $B_{cc}(r) = 0$) and broken curves also correspond to the CGHNC but the OCS treated in the RHNC approximation with a hard-sphere bridge function with optimized hard-sphere diameter.

Table 2. Thermodynamic properties for soft-core mixtures of colloid and counterions (both monovalent and divalent) with $\sigma_{cc} = 4$ nm, $\sigma_{ci} = 2.2$ nm and $\sigma_{ii} = 0.4$ nm and density of colloidal particles $\rho_c = 0.002\ \mathrm{nm}^{-3}$ (see text for details).

	60:1		60:2	
	U^{ex}/NkT	$P/\rho kT$	U^{ex}/NkT	$P/\rho kT$
CGHNC ($B_{cc} = 0$)	-6.400	0.4589	-17.223	0.1503
CGHNC ($B_{cc} = B^0$)	-8.021	0.4076	-17.194	0.0757
MD (see [27])	-8.014 ± 0.001	0.420 ± 0.001	-17.434 ± 0.001	0.260 ± 0.001
MD (this work)	-8.064	0.412	-17.303	0.259

the effective potential for a denser state, that is, further away from the non-solution boundary of the integral equation. We observe that whereas the effective potentials at high density remain repulsive at all distances, their lower-density counterparts become attractive for the states close to the non-solution line. We note that these effective potentials are not the same potentials that are extracted, for instance, from reverse Monte Carlo calculations [29]. The true OCS effective potential is given in our case by $\beta u_{\mathrm{eff}}(r)$ in equation (9) (see footnote 3). The effective potential $\beta u'_{\mathrm{eff}}(r)$, represented in figure 5, depends on the difference between the colloid–colloid bridge functions of the OCS and the multicomponent system. This difference is sometimes taken as zero [1, 12], and in that case both effective potentials, $\beta u_{\mathrm{eff}}(r)$, $\beta u'_{\mathrm{eff}}(r)$ are equal. The effective potential for the suspension 60:1, $0.002\,\mathrm{nm}^{-3}$ for the case of hard-core particles, has been obtained by Lobaskin and co-workers [29]. This potential is repulsive, in

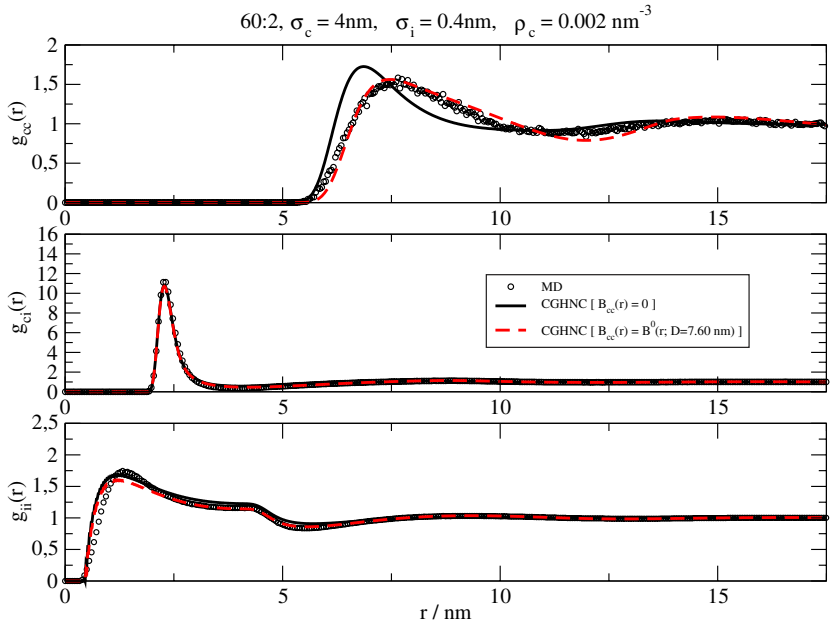

Figure 4. The same as figure 3 but for divalent counterions.

clear contrast with our $\beta u'_{\rm eff}(r)$. We expect that the $\beta u_{\rm eff}(r)$ for our soft model should be very similar to the hard-sphere case, i.e., repulsive. Therefore, this would suggest that the bridge functions, $B_{\rm cc}$ and B in equation (9), should indeed be different for the 60:1 system in the vicinity of the non-solution boundary. The dependence of $\beta u'_{\rm eff}(r)$ with the bridge functions is further supported by our results in figure 5, where we have also considered the effective potential, $\beta u'_{\rm eff}(r)$, without including the bridge function. One can see that the bridge function has a large effect on this potential, and when we do not include it in the calculation we obtain effective potentials that are basically repulsive. Therefore we would like to point out that $\beta u'_{\rm eff}(r)$ should not be taken as representative of the real effective potential but as a formal interaction that defines the OCS in the context of the CGHNC theory. Given that the real potential is expected to be in most cases repulsive, the existence of an attractive region in our $\beta u'_{\rm eff}(r)$ is indicative of a significant difference between the bridge functions of both the OCS and the multicomponent systems. On the other hand, the existence of an attractive contribution is not necessarily connected to the existence of a spinodal line. We note that the non-solution line of the integral equation does not necessarily coincide with the spinodal. This kind of behaviour is also observed in low-temperature primitive electrolytes, where the HNC non-solution line appears at temperatures much higher than the coexistence temperatures [17].

4. Bridge functions

As we have shown in the previous section and in [1], the CGHNC integral equation does not have solution when the surface charge density of the colloidal particle becomes very large or the total density decreases below a certain threshold. In order to shed light on the origin of the non-solution boundary of this type of integral equation theory, we have extracted the bridge functions of the mixture from the computer-simulated pair correlation funcions. We must bear in mind that the integral equation approach is formally exact if the bridge functions of a system

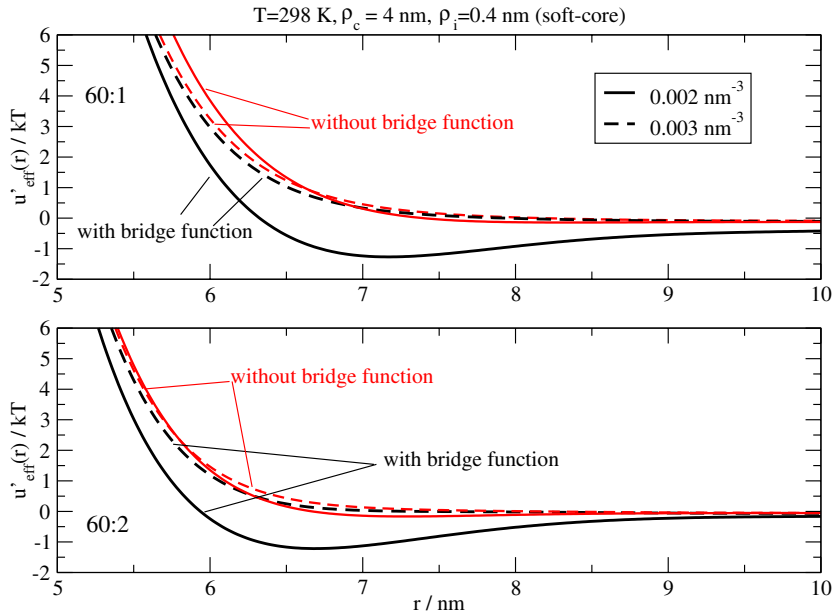

Figure 5. Effective potentials from CGHNC theory for the cases studied in figures 3 and 4 (solid curves) and for the same cases but at a higher colloidal density (broken curves). CGHNC results without the use of a bridge functions are also included in the graph.

are known. For this reason we have extracted 'empirical' bridge functions from molecular dynamics simulations for colloid + counterions mixtures.

The bridge functions were extracted from the simulated radial distribution functions using a method previously considered by one of us in electrolyte solutions [17]. The method is described here for the sake of completeness. The definition of the radial distribution function in terms of the pair potential and the bridge function,

$$g_{ij}(r) = \exp[-\beta u_{ij}(r) + h_{ij}(r) - c_{ij}(r) - B_{ij}(r)] \tag{18}$$

can in principle be used to extract the corresponding bridge functions. Since the total correlation function is known from simulation, it is straightforward to obtain the direct correlation function using the Ornstein–Zernike relation in Fourier space. Nonetheless, even for the largest interparticle distances considered here the correlation functions have not attained their asymptotic value. This fact introduces inaccuracies in the calculation of the Fourier transform of h_{ij} for small values of the wavevector, $k \to 0$. It is therefore more accurate to resort to an iterative method that combines the simulated radial distribution functions with the exact asymptotic behaviour of the direct correlation function [30].

The method considers the solution of the renormalized Ornstein–Zernike equation coupled with the closure relation:

$$\begin{aligned} h_{ij}^{\mathrm{sr}}(r) &= h_{ij}^{\mathrm{MD,sr}}(r), \qquad r \leqslant r_{\mathrm{c}} \\ c_{ij}^{\mathrm{sr}}(r) &= -\beta u_{ij}^{\mathrm{sr}}(r), \qquad r > r_{\mathrm{c}} \end{aligned} \tag{19}$$

where $h_{ij}^{\mathrm{MD,sr}}$ is the simulated short-range total correlation function, u_{ij}^{sr} is the short-range pair potential and r_{c} is a cut-off. In the context of the renormalized OZ integral equation, these short-range terms arise from the splitting of the total pair potential, $u_{ij}(r)$, into short- and

long-range parts, $u_{ij}^{\mathrm{sr}}(r) = u_{ij}(r) - u_{ij}^{\mathrm{lr}}(r)$, where

$$u_{ij}^{\mathrm{lr}}(r) = -\frac{e^2}{\varepsilon k_{\mathrm{B}} T}\frac{Z_{\mathrm{i}} Z_j}{r}(1 - \exp(-\xi r)) \tag{20}$$

ξ being an adjustable numerical parameter [31]. Similarly, the total and direct correlation functions can be written in terms of short- and long-range contributions (using matrix notation),

$$\begin{aligned} \mathbf{c}^{\mathbf{sr}}(\mathbf{r}) &= \mathbf{c}(\mathbf{r}) - \boldsymbol{\psi}(\mathbf{r}) \\ \mathbf{h}^{\mathbf{sr}}(\mathbf{r}) &= \mathbf{h}(\mathbf{r}) - \mathbf{q}(\mathbf{r}) \end{aligned} \tag{21}$$

with $\psi_{ij}(r) = -\beta u_{ij}^{\mathrm{lr}}(r)$. The long-range part of the total correlation function, $q(r)$, is related to ψ, through $\rho\hat{q}(k)\rho = \hat{v}(k) - \rho$, with $\hat{v}^{-1} = \rho^{-1} - \hat{\psi}(k)$. These short-range functions can be used to rewrite the renormalized OZ equation mentioned above (see [17]).

The bridge functions were obtained as follows. The simulated pair correlation functions were used along with the OZ relation in Fourier space, to obtain an initial guess for c^{sr}. We then solved the renormalized OZ equation along with the closure relation (19) until convergence was achieved. We found that initially we had to resort to a plain Broyles method in order to approach the initial solution to the exact one. Direct use of the Newton–Raphson method did not provide convergence. We found that the Newton–Raphson iteration can be used only when the initial guess is close enough to the final solution. The NR method failed to converge for the 60:1 case, therefore we report here results obtained only from Broyles iteration. We should point out that the extraction of the bridge function in the case of suspensions is considerably more difficult than in electrolyte solutions. Using the method described above we could not find reasonable convergent solutions for 20:1 and 60:2 suspensions. The integral equation was solved over a grid of 4096 points, with grid size 0.005 nm. Typical cut-offs, r_{c}, in equation (19), were 10, 4 and 4 nm, for colloid–colloid, colloid–ion and ion–ion correlations.

Along with the 'exact' results from simulation, we have included in the CGHNC formalism the computation of the second-order diagrams of the colloid–colloid bridge function. In other words, we have approximated the colloid–colloid bridge function in equation (17) as the sum of the following diagrams [10]:

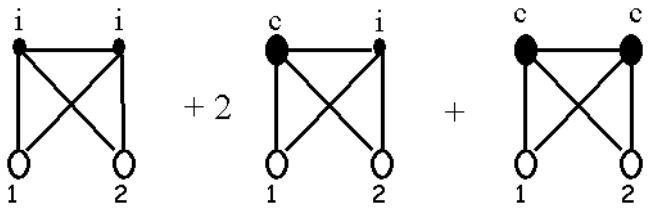

which, in this work, are expressed in terms of h-bonds [20]. This means that this kind of 'resummed' bridge function should be computed self-consistently with the colloid–colloid structure. Hence a sort of iterative procedure should be carried out in order to compute both the bridge function and the colloid–colloid radial distribution function. This procedure results in an increase of the computational time required to find a solution. Nevertheless, we found convergence in very few (three to four) iterations. We have used Gauss–Legendre quadrature with 40–100 orthogonal polynomials and 120–175 root points in the evaluation of the angular integrations involved in the computation of the diagram. On the other hand, radial integrations were evaluated using Simpson's rule with 600–700 points. A cut-off in the radial coordinate (for which the bridge function is assumed to be zero) was introduced in order to reduce computational time.

We have extracted the bridge function for two systems. First we have considered soft-core colloid + counterion mixtures with charge asymmetry 20:2 and $\sigma_{\mathrm{cc}} = 3$ nm, $\sigma_{\mathrm{ci}} = 1.7$ nm and

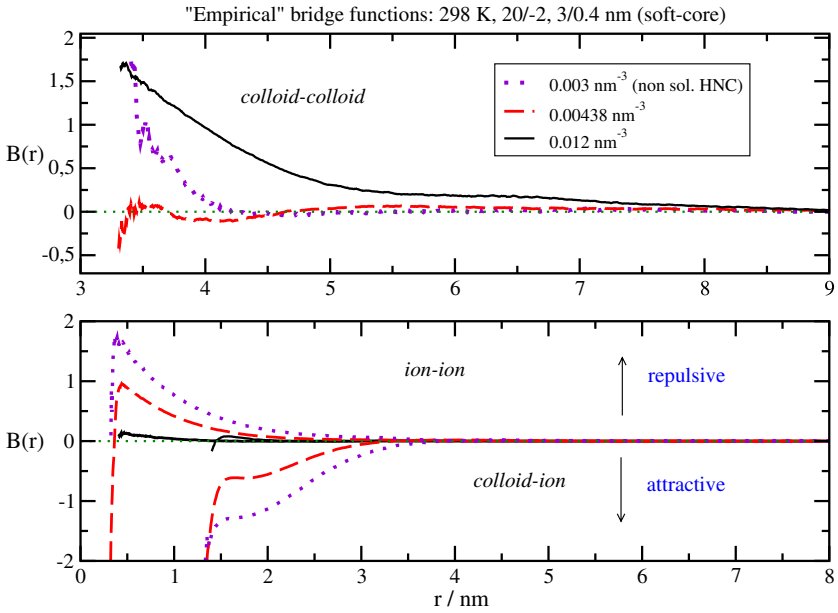

Figure 6. Bridge functions as extracted from molecular dynamics simulations for colloid + counterion mixtures with charge asymmetry 20:2 and soft-core interactions (see equation (18)) with $\sigma_{cc} = 3$ nm, $\sigma_{ci} = 1.7$ nm and $\sigma_{ii} = 0.4$ nm.

$\sigma_{ii} = 0.4$ nm. This system was already studied previously [1, 32] although 'empirical' bridge functions have not been reported. Second, we have extracted the bridge functions for the 60:1 system we have considered in the previous section. As mentioned above no convergent bridge functions were obtained for the 60:2 system.

If figure 6 the 'empirical' bridge function for the 20:2 mixture are reported for several densities, one of them located within the non-solution region of the multicomponent HNC equation (0.003 nm^{-3}). We can see that the colloid–colloid bridge function is completely repulsive for densities much larger than the non-solution boundary (0.012 nm^{-3}). Unlike the case in the high-density region, when the density is decreased, the bridge function exhibits attractive components, although this variation is not systematic. More interestingly, the colloid–ion bridge function becomes more and more attractive as the non-solution boundary is approached, whereas the ion–ion counterpart becomes more repulsive. This effect can be regarded as a sign of counterion accumulation in the vicinity of the colloidal cores. These trends are similar to the ones observed in electrolyte solutions (see [17]), implying that the origin of the behaviour observed in the suspension might be the same as that studied in electrolyte systems. What is interesting to note is that colloid–colloid bridge functions can be either attractive or repulsive, unlike ion–ion and colloid–ion bridge functions that are, respectively, repulsive and attractive.

In figures 7 and 8 the colloid–colloid 'empirical' bridge functions are compared with the hard-sphere bridge functions with optimized hard-core diameters. Also, we have included in these graphs the results obtained when the bridge function is approximated by the first (second order in density) resummed bridge diagrams. From this comparison we can conclude that neither the standard hard-sphere bridge function nor the second-order approximation of the bridge function can reproduce the attractive features that are observed in the 'empirical' bridge functions. In this regard it must be noted that the fact that the first bridge diagram

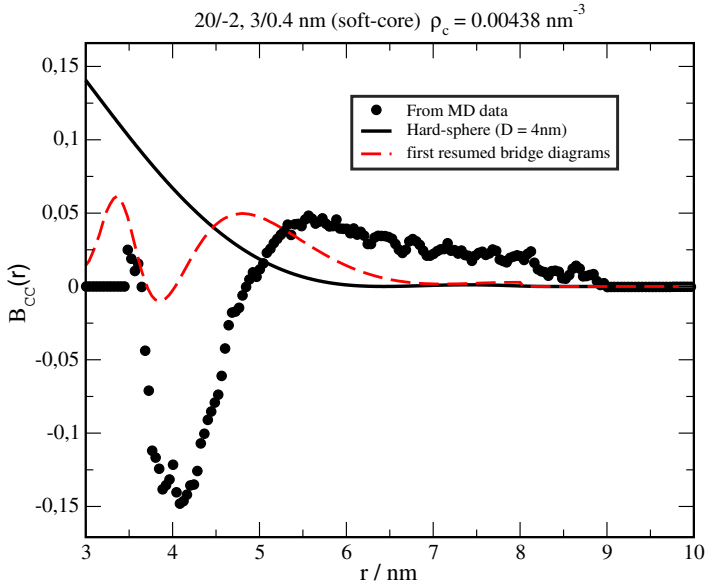

Figure 7. Colloid–colloid bridge functions for the same case considered in figure 6. In addition to the molecular dynamic results (black circles), the hard-sphere bridge function for hard-sphere diameter 4 nm and the first resummed bridge diagram are included in the graph (solid and broken curves respectively).

for this kind of system is repulsive is not new. Attard and Miklavic [33] performed accurate computations of the first resummed diagram for charged walls in the presence of a primitive model electrolyte. They found that the inclusion of the first diagram resulted in a reduction of the effective attraction between walls, precisely due to the repulsive features of the bridge function when computed in this approximation.

5. Conclusions and final remarks

In this paper we have considered the application of the CGHNC theory to charged colloidal suspensions, paying special attention to the problem of the non-solution boundary. In this regard we have shown that, due to the simplifications implicit to the CGHNC approach, this method exhibits a better numerical performance and a larger solution region than standard multi-component integral equation approaches like HNC.

As regards to the nature of the non-solution boundary, we have observed that the onset of the non-solution boundary is associated with the appearance of negative minima in our colloid–colloid effective pair potential and the occurrence of attractive features in the 'empirical' bridge functions. The minima in our effective potential is not necessarily due to the attractive nature of the bridge function, though. Actually, the attractive minimum in $\beta u'_{\mathrm{eff}}$ appears in a region where the colloid–colloid bridge function of the multicomponent system is repulsive. Further work is needed to establish a clear relation between the minima observed in this work and the differences between the bridge functions of the OCS and multicomponent systems.

The attractive features in the bridge functions, which obviously cannot be reproduced by the standard hard-sphere functions (which are repulsive by definition), do not appear either in the first diagrams of the colloid–colloid bridge function. We note that the lack of a systematic dependence with density in the colloid–colloid bridge functions precludes the development of

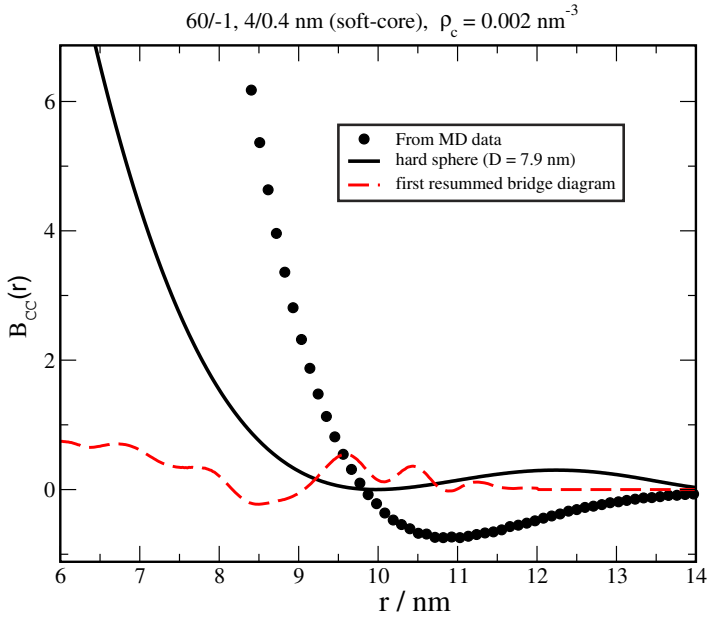

Figure 8. The same as in figure 7 but for the 60:1 soft-core system studied in figure 3.

semiempirical theories. Any attempt to extend the theory to larger surface charge densities should take into account these shortcomings. An improvement in this respect would provide the basis to describe the 'ionic condensation' effect by means of integral equation approaches.

Acknowledgments

This work has been supported by the Spanish *Dirección General de Investigación Científica y Técnica* under grant BQU2001-3615-c02-01 and *Instituto de Salud Carlos III* under grant 01/1664. FB acknowledges the use of the HPCx facility at the University of Edinburgh through the Materials Consortium (UK) and also support through EPSRC grant GR/R39726/01.

References

[1] Anta J A and Lago S 2002 *J. Chem. Phys.* **116** 10514
[2] Fennel Evans D and Wennerström H 1999 *The Colloidal Domain, where Physics, Chemistry, Biology and Technology Meet* (New York: Wiley–VCH)
Russel W B, Saville D A and Schowalter W R 1989 *Colloidal Dispersions* (Cambridge: Cambridge University Press)
[3] Derjaguin B V and Landau L D 1941 *Acta Physicoquim. URSS* **14** 633
Verwey E J W and Overbeek J Th G 1948 *Theory of the Stability of Lyophobic Colloids* (Amsterdam: Elsevier)
[4] van Roij R, Dijkstra M and Hansen J-P 1999 *Phys. Rev.* E **59** 2010
[5] Chan D Y C 2001 *Phys. Rev.* E **63** 061806
[6] Louis A A 2002 *J. Phys.: Condens. Matter* **14** 9187
[7] Caccamo C 1996 *Phys. Rep.* **274** 1
[8] Belloni L 2000 *J. Phys.: Condens. Matter* **12** R549
[9] Henderson R L 1974 *Phys. Lett.* A **49** 197
[10] Hansen J P and McDonald I R 1990 *Theory of Simple Liquids* 2nd edn (New York: Academic)
[11] Anta J A and Louis A A 2000 *Phys. Rev.* B **61** 11400

[12] Chihara J 1978 *Prog. Theor. Phys.* **59** 76
[13] Warren P 2000 *J. Chem. Phys.* **112** 4683
[14] Lozada-Cassou M, Saavedra Barrera R and Henderson D 1982 *Chem. Phys.* **77** 5150
González Tovar E and Lozada-Cassou M 1989 *J. Chem. Phys.* **93** 3761
[15] Belloni L 1998 *Colloids Surf.* A **140** 227
[16] Belloni L 1986 *Phys. Rev. Lett.* **57** 2026
[17] Bresme F, Lomba E, Weis J J and Abascal J L F 1995 *Phys. Rev.* E **51** 289
[18] Tamashiro M N, Levin Y and Barbosa M C 1998 *Physica* A **258** 341
[19] Hribar B, Kalyuzhnyi Y V and Vlachy V 1996 *Mol. Phys.* **87** 1317
[20] Perkyns J S, Dyer K M and Montgomery Pettit B 2002 *J. Chem. Phys.* **116** 9404
[21] Xu H and Hansen J-P 1998 *Phys. Rev.* E **57** 211
[22] Ashcroft N W and Langreth D C 1967 *Phys. Rev.* **156** 682
[23] Lado F 1973 *Phys. Rev.* A **8** 2548
Rosenfeld Y and Ashcroft N W 1979 *Phys. Rev.* A **20** 1208
[24] Enciso E, Lado F, Lombardero M, Abascal J L F and Lago S 1987 *J. Chem. Phys.* **87** 2249
[25] Ng K 1974 *J. Chem. Phys.* **61** 2680
[26] Broyles A A 1960 *J. Chem. Phys.* **33** 2680
[27] Lobaskin V and Linse P 2000 *J. Mol. Liq.* **84** 131
[28] Forester T R and Smith W 1996 DL_POLY Package of Molecular Simulations, CCLR
[29] Lobaskin V, Lyubartsev A and Linse P 2001 *Phys. Rev.* E **63** 020401
[30] Duh D M and Haymet A D J 1992 *J. Chem. Phys.* **97** 7716
Verlet L 1968 *Phys. Rev.* **165** 201
[31] Høye J S, Lomba E and Stell G 1992 *Mol. Phys.* **75** 1217
[32] Lobaskin V and Linse P 1998 *J. Chem. Phys.* **109** 3530
[33] Attard P and Miklavic S J 1993 *J. Chem. Phys.* **99** 6078